LRRC59 inhibits perk pathway-induced apoptosis and promotes cell proliferation, migration and invasion in colorectal cancer cells

XINGDONG HOU[1*], YUTING WANG[2*], YUZHUO CHEN[3], PEIYAN ZHONG[1], GUANGZHI WANG[4], BAICHENG LI[1], BOWEI LU[1], HANYU JIANG[5] and SHILI NING[1]

[1]Department of Gastrointestinal Surgery, The Second Affiliated Hospital of Dalian Medical University, Dalian, Liaoning 116027, P.R. China; [2]Department of Thoracic Surgery, Binzhou People's Hospital, Binzhou, Shandong 256610, P.R. China; [3]Department of Clinical Nutrition, The Second Affiliated Hospital of Dalian Medical University, Dalian, Liaoning 116027, P.R China; [4]Department of Thyroid Surgery, The Second Affiliated Hospital of Dalian Medical University, Dalian, Liaoning 116027, P.R China; [5]Department of Oncology, The First Affiliated Hospital of Dalian Medical University, Dalian, Liaoning 116000, P.R. China

Received March 31, 2025; Accepted October 13, 2025

DOI: 10.3892/or.2025.9010

Abstract. Leucine-rich repeat-containing protein 59 (LRRC59), a 244-amino-acid endoplasmic reticulum membrane protein, is implicated in the tumorigenesis of multiple malignancies. However, its functional significance in colorectal cancer (CRC) remains poorly understood. In the present study, LRRC59 expression in CRC tissues was evaluated using immunohistochemistry and western blotting. Colony formation, Cell Counting Kit-8, wound healing and Transwell assays, in *in vivo* xenograft models, were used to evaluate the effect of LRRC59 on CRC progression. Apoptosis was analyzed using flow cytometry and western blotting. The interaction between LRRC59 and the protein kinase RNA-like endoplasmic reticulum kinase (PERK) pathway was verified using the starBase database and western blotting. It was found that LRRC59 expression was significantly higher in CRC tissues than in normal tissues. LRRC59 knockdown in HCT116 and LoVo cells inhibited proliferation, migration and invasion and promoted apoptosis, and the PERK pathway was significantly activated. *In vivo* subcutaneous tumorigenesis assays corroborated these *in vitro* findings. Treatment with a PERK pathway-specific inhibitor reduced the apoptosis of HCT116 and LoVo cells with LRRC59 knockdown. These findings suggest that LRRC59 is not only significantly upregulated in CRC but also mechanistically drives tumor progression by coordinating pro-oncogenic processes, including enhanced proliferation, migration and invasion. Importantly, mechanistic evidence was provided that LRRC59 inhibits apoptosis by suppressing the PERK signaling axis, identifying this molecule a target in the development of CRC therapeutic strategies.

Correspondence to: Dr Shili Ning, Department of Gastrointestinal Surgery, The Second Affiliated Hospital of Dalian Medical University, 467 Zhongshan Road, Shahekou, Dalian, Liaoning 116027, P.R. China
E-mail: ningshili2008@163.com

*Contributed equally

Key words: colorectal cancer, leucine-rich repeat-containing protein 59, PERK pathway, endoplasmic reticulum stress, apoptosis

Introduction

Colorectal cancer (CRC) is one of the most prevalent malignancies worldwide, representing ~1/4 of all cancer diagnoses and contributing to nearly one-third of cancer-related deaths (1). New cases of CRC are expected to increase to 3.2 million and related deaths are expected to reach 1.6 million by 2040. Although most CRC cases occur in developed countries, the incidence continues to increase in developing regions (2). Despite advancements in non-invasive biomarkers for CRC diagnosis and improvements in surgery, radiotherapy and other treatments, ~50% of CRC cases are diagnosed at advanced stages, resulting in a 10% 5-year survival rate (3). Thus, identifying novel early screening markers and therapeutic targets for CRC is critical for improving early diagnosis and treatment outcomes.

Leucine-rich repeat-containing protein 59 (LRRC59) is a 244-amino acid endoplasmic reticulum (ER) membrane protein, weighing 34 kDa, that was initially identified as a ribosomal receptor in the ER (4-6). This protein is involved in the progression of various tumors. Pallai *et al* (7) observed that LRRC59 translocate from the ER to the nuclear membrane, facilitating nuclear import of CIP2A in a PP2A-independent manner, thereby promoting tumorigenesis in prostate cancer. In lung adenocarcinoma, LRRC59 is significantly overexpressed and contributes to cancer cell proliferation and invasion, which is correlated with a poor prognosis (8). Furthermore, LRRC59 is a prognostic biomarker for risk assessment in patients with urothelial carcinoma, and its elevated expression is associated with higher pathological grades. LRRC59 also regulates signaling pathways during ER stress (ERS). Depletion of LRRC59 potentiates HYOU1/XBP1-driven ERS signaling,

leading to marked inhibition of malignant cell proliferation and migration (9). These findings suggested that LRRC59 is broadly involved in tumor development and influences both apoptosis and ERS. However, the biological functions and molecular mechanisms of LRRC59 in CRC remain largely uncharacterized, and studies are needed to determine its role in CRC progression and evaluate its potential as a therapeutic target.

The ER is a specialized organelle that plays a critical role in regulating key cellular processes such as protein synthesis, folding, assembly and transport. ERS arises when misfolded or unfolded proteins accumulate within the ER, a condition triggered by factors such as ischemia, oxidative damage, and disrupted in calcium homeostasis. ERS disrupts ER homeostasis and affects cell proliferation, differentiation and apoptosis (10). A total of 3 critical sensors of ERS have been identified: protein kinase RNA-like ER kinase (PERK), inositol-requiring enzyme 1α (IRE1α), and activating transcription factor 6 (ATF6), which are all embedded in the ER membrane. Upon activation of ERS, GRP78 dissociates from these sensors and binds to misfolded or unfolded proteins, initiating the unfolded protein response (UPR) to restore ER homeostasis (11,12). However, severe or prolonged ERS can amplify protein misfolding and initiate both caspase-dependent and independent apoptotic pathways (13). In various tumor types, oncogenic factors, and metabolic and transcriptional abnormalities synergize to maintain a state of chronic ERS in tumor cells (10,14,15). Emerging research highlights a pivotal role of ERS in CRC progression, where ERS-induced activation of PERK or IRE1α through phosphorylation affects cell fate via the PERK pathway or IRE1α pathway (16,17). Therefore, the targeted modulation of ERS is a potential therapeutic approach for CRC. As LRRC59 may regulate ERS, the starBase database was screened and it was found that LRRC59 is significantly associated with key genes in the ERS PERK signaling pathway. Thus, it was hypothesized that LRRC59 affects CRC progression by regulating the PERK signaling pathway.

The present results demonstrated that LRRC59 was overexpressed in CRC, leading to the promotion of cell proliferation, migration and invasion and inhibition of apoptosis. Additionally, LRRC59 inhibited apoptosis by mitigating PERK signaling.

Materials and methods

Tissue sample collection. CRC tissues and their corresponding adjacent normal tissue samples were obtained from six patients who underwent surgical procedures (July 2024-December 2024) at the Second Affiliated Hospital of Dalian Medical University (Dalian, China). This was an opportunistic cohort. Detailed clinical and pathological data for these patients are summarized in Table I [five males and one female, with a median age of 69.5 years (range 65-80)]. Written informed consent was obtained for the use of the tissue samples, and the study was approved by the Ethics Committee of the Second Affiliated Hospital of Dalian Medical University (approval no. KY2024-136-01; Dalian, China). The limited specimen availability reflects the stringent inclusion criteria: i) Signed patient informed consent, ii) confirmed CRC diagnosis and iii) tissue quality sufficient for immunohistochemical (IHC) and western blot analysis. While it is recognized that this precluded formal power calculations, the present sample size is consistent with exploratory translational studies (18,19) and yielded statistically significant results across key endpoints: Animal model outcomes, clinical specimen IHC analysis and protein expression profiling. It is acknowledged that larger samples would strengthen these findings and will address this in future validation studies.

Cell culture and transfection. The CRC cell lines HCT116 and LoVo, purchased from Suzhou HyCyte™ Biotechnology Co., Ltd., were cultured in RPMI-1640 medium (cat. no. 11875119; Gibco; Thermo Fisher Scientific, Inc.) supplemented with 10% fetal bovine serum (cat. no. A5670701; Gibco; Thermo Fisher Scientific, Inc.) and 1% penicillin-streptomycin (cat. no. SC118; Seven Innovations Biological Technology Co., Ltd). The cells were maintained at 37˚C in a 5% CO_2 atmosphere. The PERK inhibitor GSK (cat. no. HY-13820; MedChemExpress) was added to HCT116 and LoVo cells for 12 h (1 μM). After the cells reached ~50% confluency, LRRC59-small interfering RNA (siRNA) (20 μM) was transfected (37˚C) with Lipofectamine 3000 (cat. no. L3000015; Thermo Fisher Scientific, Inc.), and the cells were harvested after 24 or 48 h for reverse transcription-quantitative polymerase chain reaction (RT-qPCR) and western blotting. LRRC59-siRNA constructs were designed by Suzhou GenePharma Co., Ltd., and siNC was used as a negative control. The sequences were as follows: si-LRRC59-1: 5'-GACUACUCUACCGUCGGAUTT-3'; si-LRRC59-2: 5'-GUGCAAACAAGGUGUUACATT-3'; and si-NC: 5'-UUC UCCGAACGUGUCACGUTT-3'. The 293T cell line used in the present study was purchased from the Cell Bank of the Chinese Academy of Sciences. The cells were cultured in DMEM medium (cat. no. PM150210; Procell Life Science & Technology Co., Ltd.) supplemented with 10% fetal bovine serum (cat. no. A5670701; Gibco; Thermo Fisher Scientific, Inc.) and 1% penicillin-streptomycin (cat. no. SC118; Seven Innovations Biological Technology Co., Ltd). All cells were maintained at 37˚C in a humidified incubator with 5% CO_2 and were used for subsequent lentiviral transduction.

Stable transgenic cells via short hairpin RNA lentiviral transduction. Stable LRRC59-knockdown LoVo cells were constructed using 3rd-generation lentiviral vectors. The short hairpin RNA-expressing plasmid pLV3-H1/GFP&Puro-shLRRC59 (target sequence: 5'-CTG GATCTGTCTTGTAATAAA-3') and non-targeting control sh-NC (5'-TTCTCCGAACGTGTCACGT-3') were obtained from Suzhou GenePharma Co., Ltd. Viral particles were packaged in 293T cells (Cell Bank of the Chinese Academy of Sciences) by co-transfecting the transfer plasmid with packaging plasmids pGag/Pol, pRev, and pVSV-G (GenePharma Co., Ltd.) at a mass ratio of 4:2:1:1 using RNAi-Mate transfection reagent (cat. no. G04001; GenePharma Co., Ltd.). Transfection complexes were incubated with the cells in 15-cm dishes for 6h at 37˚C in a 5% CO_2 atmosphere, followed by replacement of the medium with complete medium. Viral supernatants were harvested 72 h post-transfection, filtered through 0.45-μm membranes, and concentrated via ultracentrifugation (32,000 x g, 2 h, 4˚C). LoVo cells were transduced

Table I. Specific details of the patients.

Number	Age, years	Sex	Clinical information	Pathological information
1	68	Male	pT2N0M0	Colonic moderately differentiated adenocarcinoma
2	67	Male	pT3N0M0	Moderately differentiated adenocarcinoma of the rectum
3	75	Male	pT4N0M0	Moderately differentiated adenocarcinoma of the rectum
4	71	Male	pT2N0M0	Colonic moderately differentiated adenocarcinoma
5	65	Female	pT3N0M0	Colonic moderately differentiated adenocarcinoma
6	80	Male	pT2N0M0	Colonic moderately differentiated adenocarcinoma

with viral stocks at a multiplicity of infection of 10 in the presence of 5 μg/ml Polybrene (cat. no. H9268; MilliporeSigma) for 24 h at 37˚C, after which the medium was refreshed. Stable populations were selected with 2 μg/ml puromycin (cat. no. HY-B1743; MedChemExpress) for 7 days, followed by maintenance in 1 μg/ml puromycin. Knockdown efficiency was validated by western blotting.

RT-qPCR. Total RNA was isolated using RNAkey™ Total RNA Extraction Reagent (cat. no. SM139-02; Seven Innovations Biological Technology Co., Ltd.). cDNA was synthesized using a two-step RT-qPCR kit (cat. no. SRQ-01; Seven Innovations Biological Technology Co., Ltd.) as follows: 50˚C for 8 min and 85˚C for 5 sec. Real-time PCR amplification of the cDNA templates was performed using a Two-Step RT and qPCR Kit (cat. no. SRQ-01; Seven Innovations Biological Technology Co., Ltd.) on a QuantStudio™ 5 system (Thermo Fisher Scientific, Inc.). The thermocycling conditions were as follows: 95˚C for 30 sec; 40 cycles at 95˚C for 20 sec, and 60˚C for 20 sec. The $2^{-\Delta\Delta Cq}$ method was used to calculate the relative mRNA expression (20). GAPDH was used as an internal control. The primer sequences were as follows: LRRC59 forward, 5'-CCTTGCCTGTCAGCTTTGC-3' and reverse, 5'-TCATGTGCTGTAACACCTTGTTTG-3'; and GAPDH forward, 5'-CATGTTCGTCATGGGTGTGAA-3' and reverse, 5'-GGCATGGACTGTGGTCATGAG-3'.

Cell Counting Kit-8 (CCK-8) assay. CRC cells were transfected with either si-LRRC59 or si-NC. After 24 h incubation cell counts were determined, and the cells were seeded into 96-well plates ($5x10^3$ cells/well). Following incubation for 24, 48 and 72 h, fresh medium containing 10% CCK-8 reagent (cat. no. SC119; Seven Innovations Biological Technology Co., Ltd.) was added. After 2 h, optical density was measured at 450 nm.

Colony formation assay. CRC cells were transfected with either si-LRRC59 or si-NC for 24 h. After counting, the cells were seeded into 6-well plates ($1x10^3$ cells/well). The plates were maintained in culture for one week. Colonies (contains at least 50 cells) were fixed with 10% methanol (15 min at room temperature) and stained with 0.1% crystal violet (30 min at room temperature) to enhance visualization.

Scratch wound healing assay. CRC cells were transfected with si-LRRC59 or si-NC, seeded into 6-well plates, and cultured to 90% confluence. Scratch wounds were created using a sterile 10-μl pipette tip, and cellular debris was removed by washing with phosphate-buffered saline (PBS). Basal medium (without serum) was added, and images of the scratch areas were captured and measured at both 0 h and 48 h using a Leica microscope (inverted light microscope). Wound closure percentages were analyzed using ImageJ 1.54d software (National Institutes of Health).

Migration and invasion assays. Cells ($1x10^5$ cells/well) were plated into 24-well 8-μm pore size Transwell chambers (cat. no. 3422; Corning, Inc.), with or without Matrigel (cat. no. 354230; Corning, Inc.) coating (37˚C, 6 h). The lower chambers contained basal medium with 10% fetal bovine serum as a chemoattractant. After 48 h, migratory cells were fixed in methanol (1 h at room temperature) and stained with 0.1% crystal violet (20 min at room temperature). A total of 5 random fields were selected for analyses.

IHC analysis. CRC tissues, adjacent normal tissues, and xenograft tumor sections (4-μm thickness) underwent sequential deparaffinization in xylene and rehydration in a graded ethanol series at room temperature. Following antigen retrieval in Tris/EDTA buffer (pH 9.0), endogenous peroxidase activity was quenched by adding 3% H_2O_2 incubation (10 min incubation, room temperature). The sections were rinsed three times with distilled water (5 min/wash) and equilibrated in PBS for 5 min. After blocking with 5-10% normal goat serum (cat. no. G1208-5ML; Servicebio Technology Co., Ltd.) for 10 min at room temperature, the sections were incubated overnight at 4˚C with the following primary antibodies: anti-LRRC59 (1:200; cat. no. 27208-1-AP; Proteintech Group, Inc.), anti-GRP78 (1:200; cat. no. 11587-1-AP; Proteintech Group, Inc.), anti-p-PERK (1:300; cat. no. PA5-40294; Invitrogen), anti-ATF4 (1:200; cat. no. 28657-1-AP; Proteintech Group, Inc.), and anti-CHOP (1:200; cat. no. 15204-1-AP; Proteintech). Next, horseradish peroxidase-conjugated secondary antibody (1:200; cat. no. G1213; Servicebio Technology Co., Ltd.) was incubated with the sections at 37˚C for 1 h. A DAB Chromogenic Kit cat. no. G1212; Wuhan Servicebio Technology Co., Ltd.) was used to treat the sections for 15 min, followed by hematoxylin counterstaining (cat. no. G1004; Servicebio Technology Co., Ltd.) for 3 min at room temperature and bright-field microscopy using a Leica DMI1 system. The staining intensity and percentage were quantified using the H-score formula: H-score=$\sum$(pi x i), where pi is the percentage of positive pixels and i is the intensity grade.

Western blotting and antibodies. Proteins were extracted from tissues and cells using cell lysis buffer for western blotting and immunoprecipitation (IP; cat. no. P0013; Beyotime Institute of Biotechnology) containing phenyl-methyl-sulphonyl-fluoride (cat. no. SW107; Seven Innovations Biological Technology Co., Ltd.) and phosphatase inhibitors (cat. no. SW106; Seven Innovations Biological Technology Co., Ltd.). The protein concentration was quantified using the BCA assay (cat. no. KGB2101; Nanjing KeyGen Biotech Co., Ltd.). Precast polyacrylamide gels (7.5-12.5%; cat. no. SW145; Seven Innovations Biological Technology Co., Ltd) were loaded with 20 μg protein per lane along with pre-stained protein molecular weight markers (cat. no. SW176; Seven Innovations Biological Technology Co., Ltd.). Electrophoresis was performed at 80 V for 30 min followed by 120 V for 60-90 min, followed by wet transfer (300 mA, 30 min) onto polyvinylidene fluoride membranes (cat. no. ISEQ00005; MilliporeSigma). The membranes were blocked with 5% non-fat milk in Tris-buffered saline containing 0.1% Tween-20 at room temperature for 1 h, followed by incubation with primary antibodies overnight at 4˚C. The following primary antibodies were used: β-tubulin (1:10,000; cat. no. AP0064; Bioworld Technology, Inc.), LRRC59 (1:10,000; cat. no. 27208-1-AP; Proteintech Group, Inc.), GRP78 (1:10,000; cat. no. 11587-1-AP; Proteintech Group, Inc.), PERK (1:1,000; cat. no. 24390-1-AP; Proteintech Group, Inc.), phosphorylated PERK (p-PERK) (1:1,000; cat. no. AP1501; ABclonal Biotech Co., Ltd.), ATF4 (1:10,000; cat. no. 81798-1-RR; Proteintech Group, Inc.), p-EIF2α (1:1,000; cat. no. AP0692; ABclonal Biotech Co., Ltd.), EIF2α (1:10,000; cat. no. 82936-1-PBS; Proteintech Group, Inc.), CHOP (1:1,000; cat. no. 15204-1-AP; Proteintech Group, Inc.), Caspase 3 (1:1,0000; cat. no. 82202-1-RR; Proteintech Group, Inc.), active-caspase-3 (1:1,000; cat. no. A11021; ABclonal Biotech Co., Ltd.), Bax (1:1,000; cat. no. A19684; ABclonal Biotech Co., Ltd.), Bcl-2 (1:1,000; cat. no. A19693; ABclonal Biotech Co., Ltd.). Horseradish peroxidase-conjugated rabbit secondary antibodies (1:2,000; cat. no. AS014; Abcam) and mouse secondary antibodies (1:2,000; cat. no. AS003; ABclonal Biotech Co., Ltd.) were applied for 1 h at room temperature. Protein signals were detected using Super ECL Reagent (cat. no. 36208ES60; Shanghai Yeasen Biotechnology Co., Ltd.) and visualized using a ChemiDoc Imaging System (Bio-Rad Laboratories, Inc.). Quantitative analysis was performed using ImageJ 1.54d software. All experiments were conducted in triplicate.

Flow cytometry. HCT116 and LoVo cells ($5x10^4$) were stained using an Annexin V-FITC/PI Apoptosis Detection Kit (cat. no. 40302ES50; Shanghai Yeasen Biotechnology Co., Ltd.). The cells were trypsinized using 0.25% ethylene-diamine-tetraacetic acid-free trypsin (cat. no. SC108, Seven Innovations Biological Technology Co., Ltd.) and pelleted by centrifugation at 300 x g for 5 min at 4˚C. After two washes with ice-cold PBS (centrifugation: 300 x g, 4˚C, 5 min), $5x10^5$ cells were resuspended in 100 μl 1X Annexin V Binding Buffer. Subsequently, 5 μl FITC-conjugated Annexin V and 10 μl propidium iodide working solution (20 μg/ml) were added, followed by gentle vortexing and 15 min incubation in light-protected conditions at room temperature. The reaction was terminated by adding 400 μl ice-cold binding buffer. The samples were maintained on ice and analyzed within 60 min using a NovoCyte Advanteon flow cytometer (Agilent Technologies, Inc.). Apoptosis levels were assessed using NovoExpress software (version 1.6.2; Agilent). All experiments were conducted in triplicate.

Xenograft tumor formation. Female BALB/c female mice (aged 5 weeks; n=10; weight, 18.23±0.74 g) were acquired from Beijing Vital River Laboratory Animal Technology Co., Ltd. The mice were housed in a specific pathogen-free grade animal room in individually ventilated cages within the barrier at a rate of five mice per cage. The mice were housed under controlled environmental conditions (26-28˚C, 40-60% humidity) with a standardized 10 h light/14 h dark photoperiod. All mice had unrestricted access to standard laboratory chow and water throughout the study period, along with environmental enrichment (for example, nesting materials and shelters). The specific humane endpoint criteria implemented in the experiment were as follows: i) The tumor volume of any single tumor did not exceed 2,000 mm^3; ii) Tumor ulceration or necrosis: Progressive ulceration, severe necrosis, or infection of the tumor surface was expected to be irreversible or cause significant pain; iii) weight loss: Mice lost more than 20% of their initial weight within three consecutive days; iv) activity status and behavioral changes: Mice exhibited severely reduced activity, hunchbacks, coarse and messy fur, difficulty breathing, inability to access food or water normally, and other significant signs of pain or impending death; v) Functional impairment caused by tumors: Tumor growth significantly impaired the mobility (such as walking) and normal physiological functions of mice; and vi) monitoring and execution: Trained researchers observed the experimental animals at least once daily. Mice were monitored for any potential signs of humane endpoints twice a day.

When a mouse met any of the humane endpoint criteria aforementioned, it was euthanized immediately. The maximum tumor volume was 1372.24 mm^3 and the maximum tumor diameter was 16.14 mm.

All procedures were approved by the Institutional Animal Care and Use Committee of Wuhan Servicebio Technology Co., Ltd. (approval no. 2024167). The experiments strictly adhered to the institution's guidelines for animal welfare and use. The mice were randomly assigned to two groups with five animals per group. Each mouse received a subcutaneous injection of LoVo cells ($1x10^7$ cells) that had been transfected with either sh-NC or shLRRC59, resuspended in 100 μl of PBS. Tumor volumes were measured at 3-day intervals, and the tumors were excised and weighed after 34 days. Mice were anesthetized by intraperitoneal injection of 2% tribromoethanol (20 ml/kg), and deep anesthesia was confirmed by the absence of a pedal reflex. Euthanasia was induced via cervical dislocation. No experimental procedures were performed on the mice after tribromoethanol anesthesia.

Our sample size decisions were guided by both field-specific standards and ethical considerations. Animal studies (n=5/group): this sample size aligns with established norms for xenograft tumor models in published literature (21,22). Consistent with the 3R principles (Replacement, Reduction, Refinement) under international animal research guidelines,

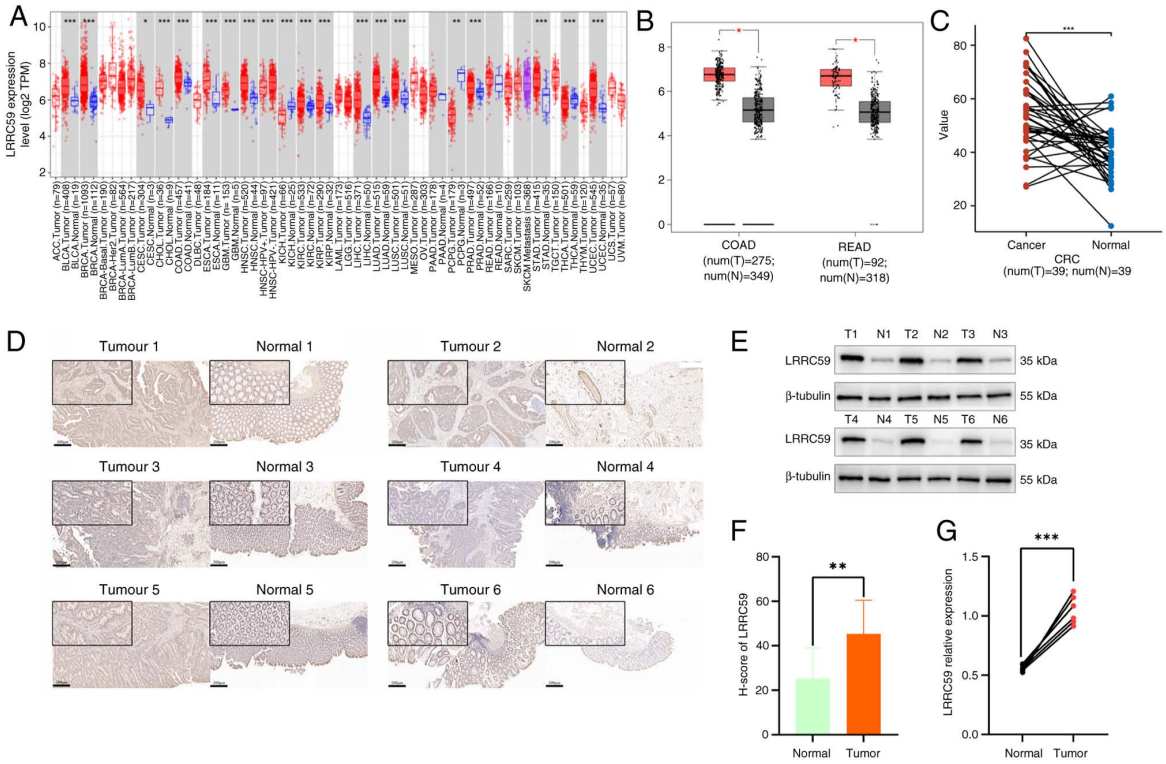

Figure 1. LRRC59 upregulation in CRC tissues. (A-C) mRNA expression of LRRC59 in CRC tissues was analyzed using (A) the TIMER2.0, (B) GEPIA and (C) The Cancer Genome Atlas databases. (D) Immunohistochemistry and (F) H-score of LRRC59 in normal versus CRC tissues. (E and G) Western blot analysis of LRRC59 protein in CRC and normal tissues. Scale bars, 50 and 200 μm. *P<0.05, **P<0.01 and ***P<0.001. CRC, colorectal cancer; COAD, colon adenocarcinoma; READ, rectum adenocarcinoma.

group sizes were optimized to minimize animal use while maintaining experimental validity.

The choice of the LoVo cell line for *in vivo* studies was based on: Literature-established protocols: Subcutaneous xenograft models using LoVo are well-documented for CRC studies (23,24). Ethical optimization: This approach minimized animal usage while maintaining experimental validity, consistent with 3R principles. Biological rationale: Complementary *in vitro* experiments demonstrated consistent LRRC59 effects across both HCT116 and LoVo cell lines. Critically, our dual-cell-line validation confirmed that LRRC59's modulation of the PERK pathway occurs independently of cellular context. LoVo cells were therefore selected for *in vivo* validation as they represent a mechanistically conserved model of LRRC59 function in CRC progression.

Mice were euthanized on Day 34 for two reasons: i) Tumor size limits: IACUC protocol requires euthanasia before tumor volume exceeds 2,000 mm^3. Projected growth curves indicated most mice would reach this threshold by Day 34. ii) Humane endpoints: Mice were monitored daily for distress signs (for example, >20% weight loss, lethargy, ulceration). Any mouse meeting these criteria was euthanized immediately; none required early euthanasia before Day 34. This schedule preempted welfare violations while allowing meaningful cross-group comparison at a standardized endpoint.

Blinding method. Blinding was applied to evaluate the results during the measurement phase of all experiments involving subjective evaluation.

Statistical analysis. Data are expressed as the mean values accompanied by standard deviations calculated from three independent experiments. Statistical analyses were conducted using GraphPad Prism 8.0 software (GraphPad, Inc.; Dotmatics). For comparisons between two groups, two-tailed, paired Student's t-test was used, whereas one-way analysis of variance was used to analyze multiple groups. Normality was assessed using the Shapiro-Wilk test for all experimental groups, with results indicating P>0.05 for each dataset, confirming adherence to normality assumptions. Prior to ANOVA, homogeneity of variance was further verified using Levene's test (P>0.05), confirming that all ANOVA prerequisites were satisfied. For comparisons across the three groups (including controls), Dunnett's post hoc test was applied. All pairwise comparisons against the control group showed statistically significant differences (P<0.05). Statistical significance thresholds were set at *P<0.05, **P<0.01 and ***P<0.001.

Results

Elevated expression of LRRC59 in CRC tissues. To evaluate the LRRC59 expression in CRC tissues in compared with that in normal tissues, mRNA expression levels were initially analyzed using the TIMER2.0 database (http://timer.comp-genomics.org/) (Fig. 1A). The results revealed significantly higher LRRC59 mRNA levels in colon adenocarcinoma tissues than in normal tissues. Further data were acquired from both paired and unpaired CRC samples using the GEPIA (http://gepia.cancer-pku.cn/index.html) (Fig. 1B) and TCGA

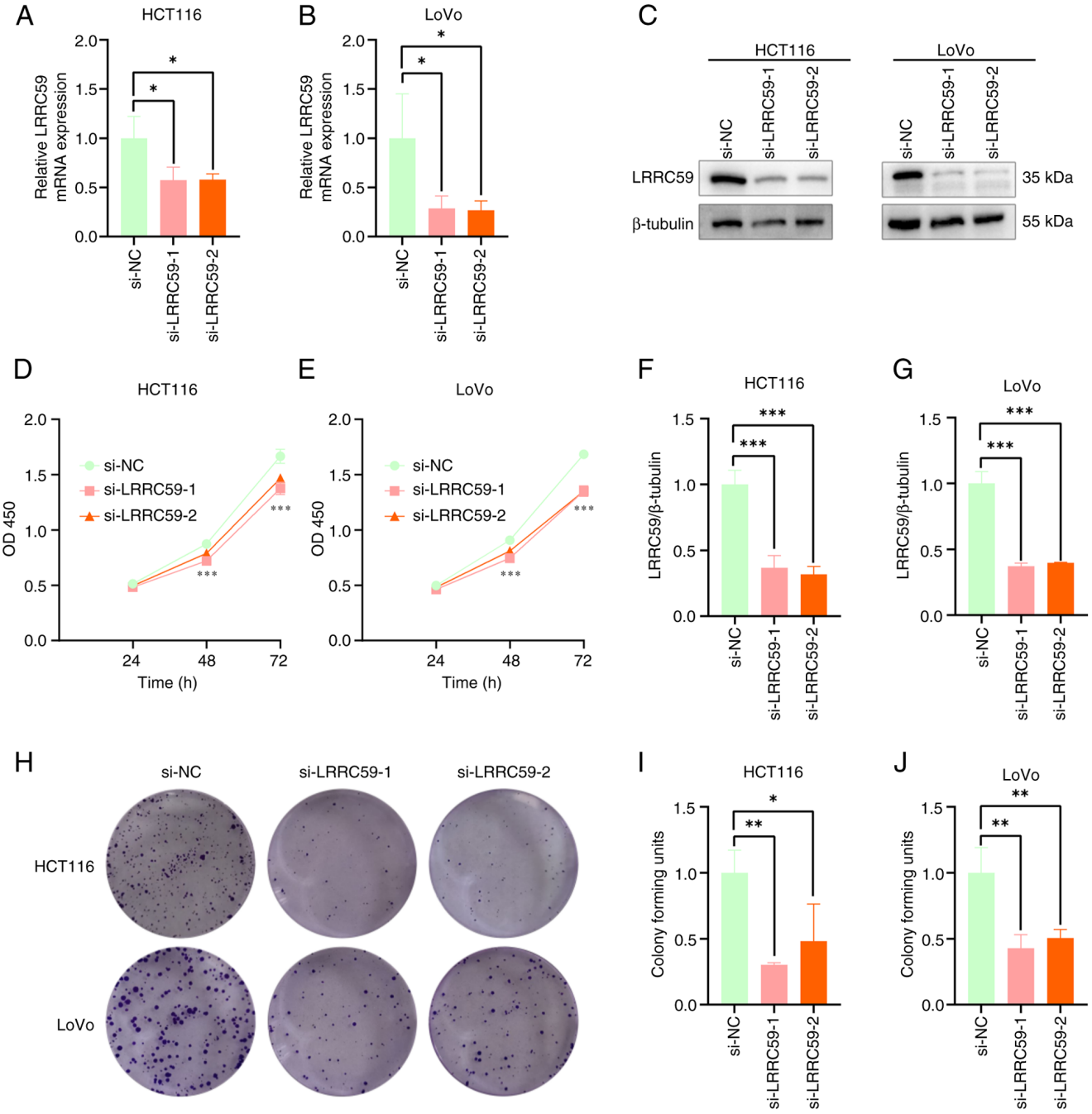

Figure 2. LRRC59 enhances CRC cell proliferation. (A and B) Efficiency of si-LRRC59 transfection in HCT116 and LoVo cells confirmed by reverse transcription-quantitative PCR. (C, F and G) Western blot analysis of LRRC59 expression in si-NC and si-LRRC59 transfected cells. (D and E) Cell proliferation rates were evaluated using the Cell Counting Kit-8 assay on days 1, 2, and 3 following transfections. (H-J) Colony formation assays evaluating the tumorigenic potential of CRC cells. *P<0.05, **P<0.01 and ***P<0.001. CRC, colorectal cancer; si-, small interfering; NC, negative control.

databases (https://www.tcpaportal.org/) (Fig. 1C), respectively. Statistical analyses showed that LRRC59 mRNA expression was markedly upregulated in CRC tissues compared with that in corresponding adjacent normal tissues. To substantiate these results, CRC and adjacent normal tissues from six patients were analyzed using IHC (Fig. 1D and F) and western blotting (Fig. 1E and G). The results revealed a significant increase in LRRC59 protein expression in CRC tissues compared with that in their normal tissue counterparts. Collectively, these findings indicated that LRRC59 is substantially overexpressed in CRC tissues compared with in normal paracancerous tissues.

LRRC59 knockdown suppresses CRC cell proliferation. The function of LRRC59 in promoting CRC cell proliferation was examined by silencing its expression in HCT116 and LoVo cell lines using siRNA. RT-qPCR (Fig. 2A and B) and western blot analysis (Fig. 2C-E) confirmed the successful silencing of LRRC59. Cell viability and proliferation potential were detected using the CCK-8 (Fig. 2F and G) and colony formation assays (Fig. 2H-J). These results revealed reduced colony formation and inhibition of cell proliferation following LRRC59 knockdown. These findings suggested that LRRC59 promotes CRC cell proliferation.

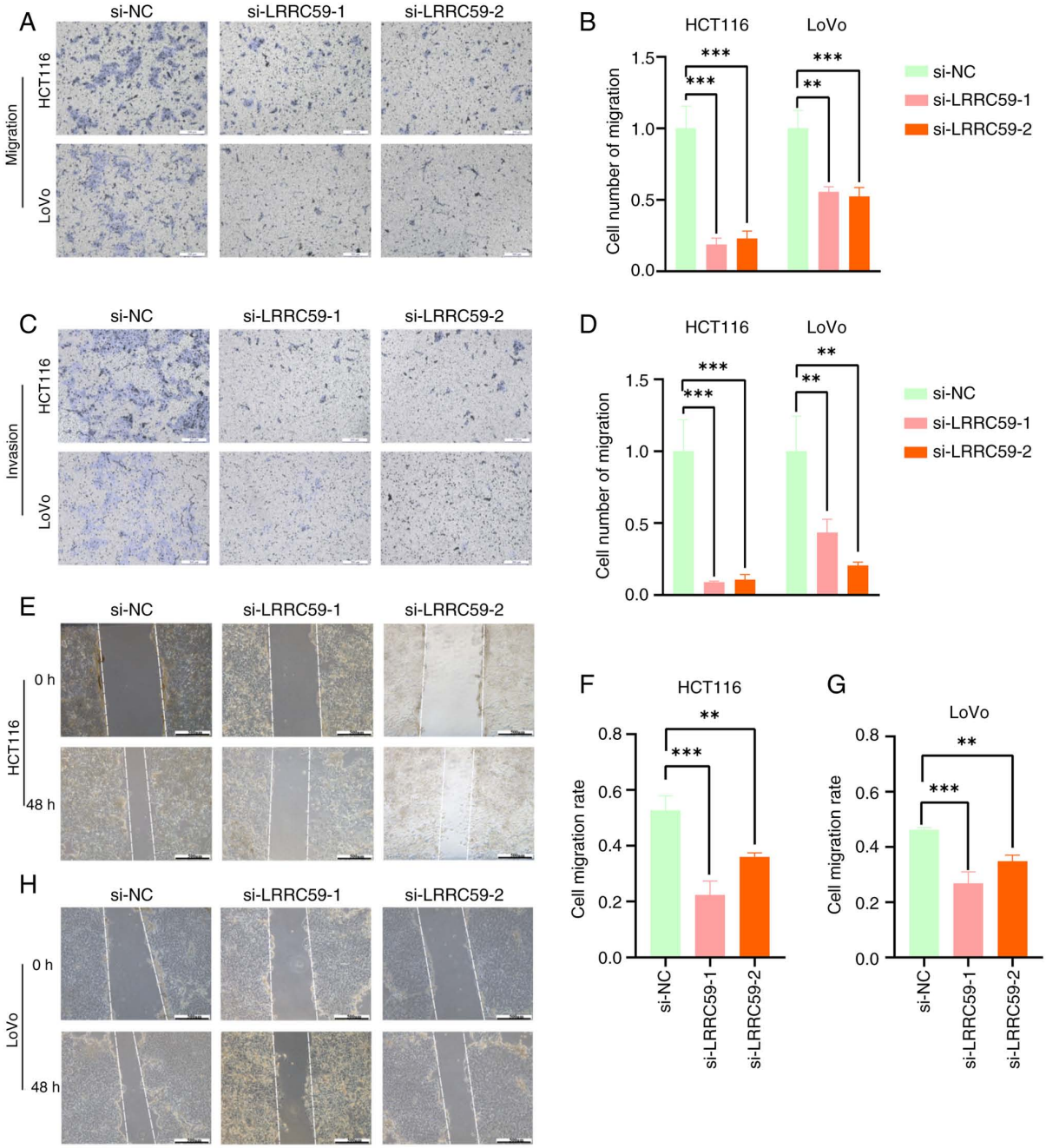

Figure 3. LRRC59 facilitates migration and invasion in colorectal cancer cells. (A, B and E-H) Migratory potential evaluated using Transwell and wound healing assays. (C and D) Invasive capacity was assessed through Transwell assays with Matrigel. Scale bars, 200 and 500 μm. **P<0.01 and ***P<0.001. si-, small interfering; NC, negative control.

Silencing LRRC59 reduces CRC cell migration and invasion. The effect of LRRC59 on CRC cell migration and invasion was evaluated using Transwell and wound healing assays. LRRC59 silencing significantly reduced the number of cells that migrated through the porous membrane or Matrigel-coated inserts (Fig. 3A-D). Similarly, wound healing assays revealed diminished motility in cells with reduced LRRC59 expression (Fig. 3E-H). These results highlighted the role of LRRC59 in promoting CRC cell migration and invasion.

Knockdown of LRRC59 induces activation of the PERK pathway in CRC cells. Emerging evidence suggests that LRRC59 is involved in ERS regulation (9). Bioinformatics analysis using the starBase database (http://starbase.sysu.edu.cn/) revealed a significant positive correlation between LRRC59 and GRP78 (HSPA5), a master chaperone of ERS. These results suggested that LRRC59 modulates ERS signaling, implicating a regulatory role in CRC pathogenesis. The potential associations between LRRC59 and key regulatory components of the three UPR branches were subsequently examined: IRE1α, PERK and ATF6 pathways. The results revealed a significant association between LRRC59 and PERK signaling pathways (ATF4 and CHOP) (Fig. 4A). To validate these findings, LRRC59 in HCT116 and LoVo cells was knocked down, followed by western blot analysis of PERK pathway components. Altered expression of PERK

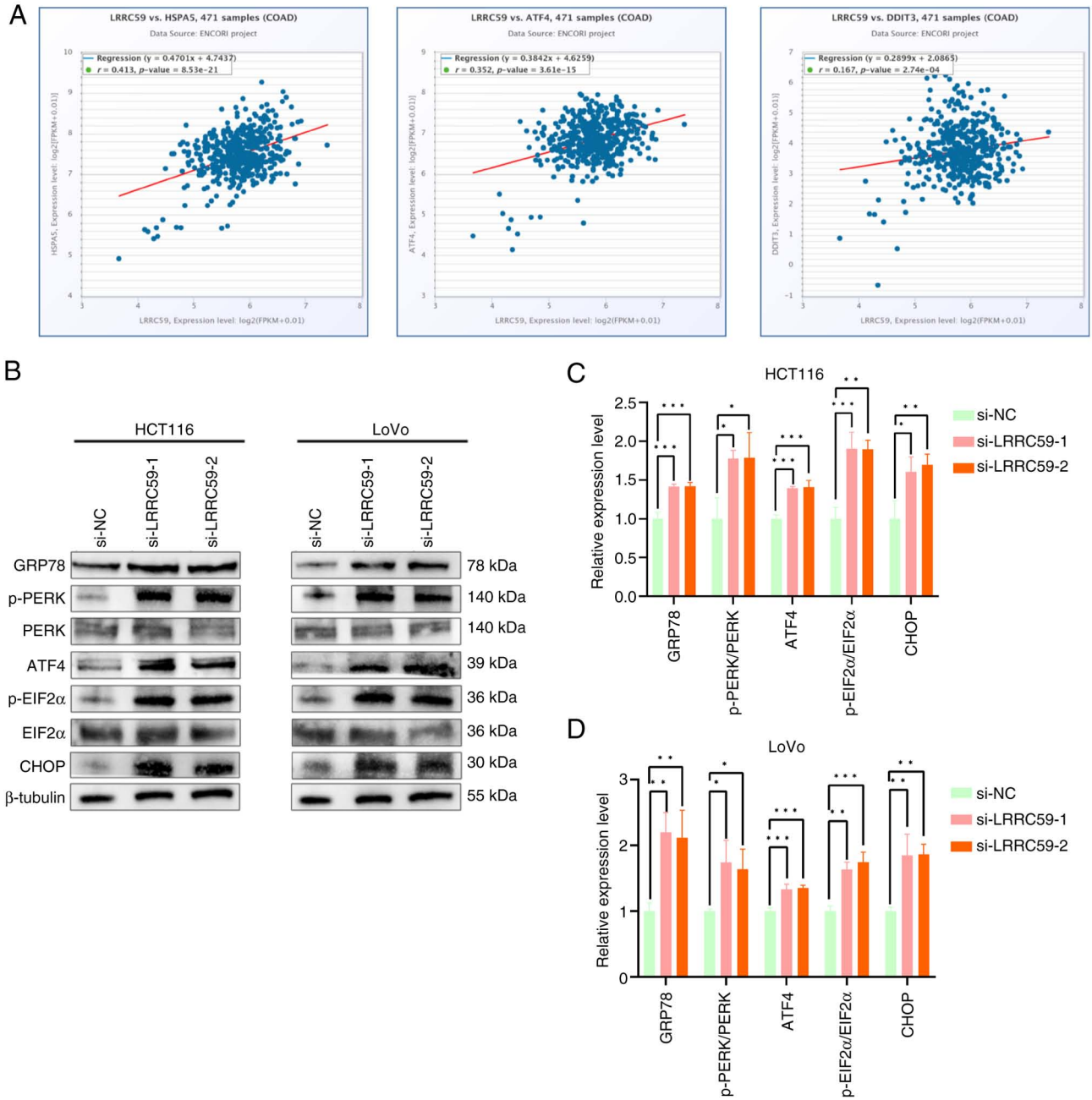

Figure 4. LRRC59 regulates the PERK-mediated ERS signaling pathway. (A) According to the starBase database, LRRC59 is associated with ERS pathway key genes GRP78, ATF4, and CHOP in colorectal cancer. (B-D) Western blot analysis of PERK pathway-related proteins (GRP78, p-PERK, PERK, ATF4, p-EIF2α, EIF2α and CHOP). *P<0.05, **P<0.01 and ***P<0.001. ER, endoplasmic reticulum; PERK, protein kinase RNA-like ER kinase; ERS, ER stress; p-, phosphorylated; si-, small interfering; NC, negative control; COAD, colon adenocarcinoma.

pathway-related proteins was observed, including increased levels of GRP78, p-PERK, p-EIF2α, ATF4 and CHOP, in LRRC59-silenced cells (Fig. 4B-D). These data demonstrated that LRRC59 is a negative regulator of PERK-mediated ERS signaling in CRC cells.

LRRC59 suppresses apoptosis in CRC cells. ERS plays a critical role in modulating apoptosis (25-27). To investigate whether LRRC59 regulates apoptosis through ERS pathways, apoptotic responses were first examined following LRRC59 knockdown. Flow cytometric analysis demonstrated that LRRC59 deficiency in HCT116 and LoVo cells resulted in a substantial increase in apoptotic cells compared with that in control cells (Fig. 5A-D). Western blot analysis of apoptosis-related proteins (Fig. 5E-G) demonstrated upregulation of active caspase-3 and decreased Bcl-2 and Caspase3 expression. These findings provided further evidence that LRRC59 functions as an anti-apoptotic factor in CRC cells.

LRRC59 modulates apoptosis via PERK signaling in CRC. Increased PERK phosphorylation is a hallmark of PERK pathway activation. To assess whether LRRC59 influenced apoptosis by regulating the PERK pathway, LRRC59 knockdown CRC cells were treated with GSK, a PERK pathway inhibitor. The results showed that GSK treatment significantly inhibited PERK phosphorylation. Western blot

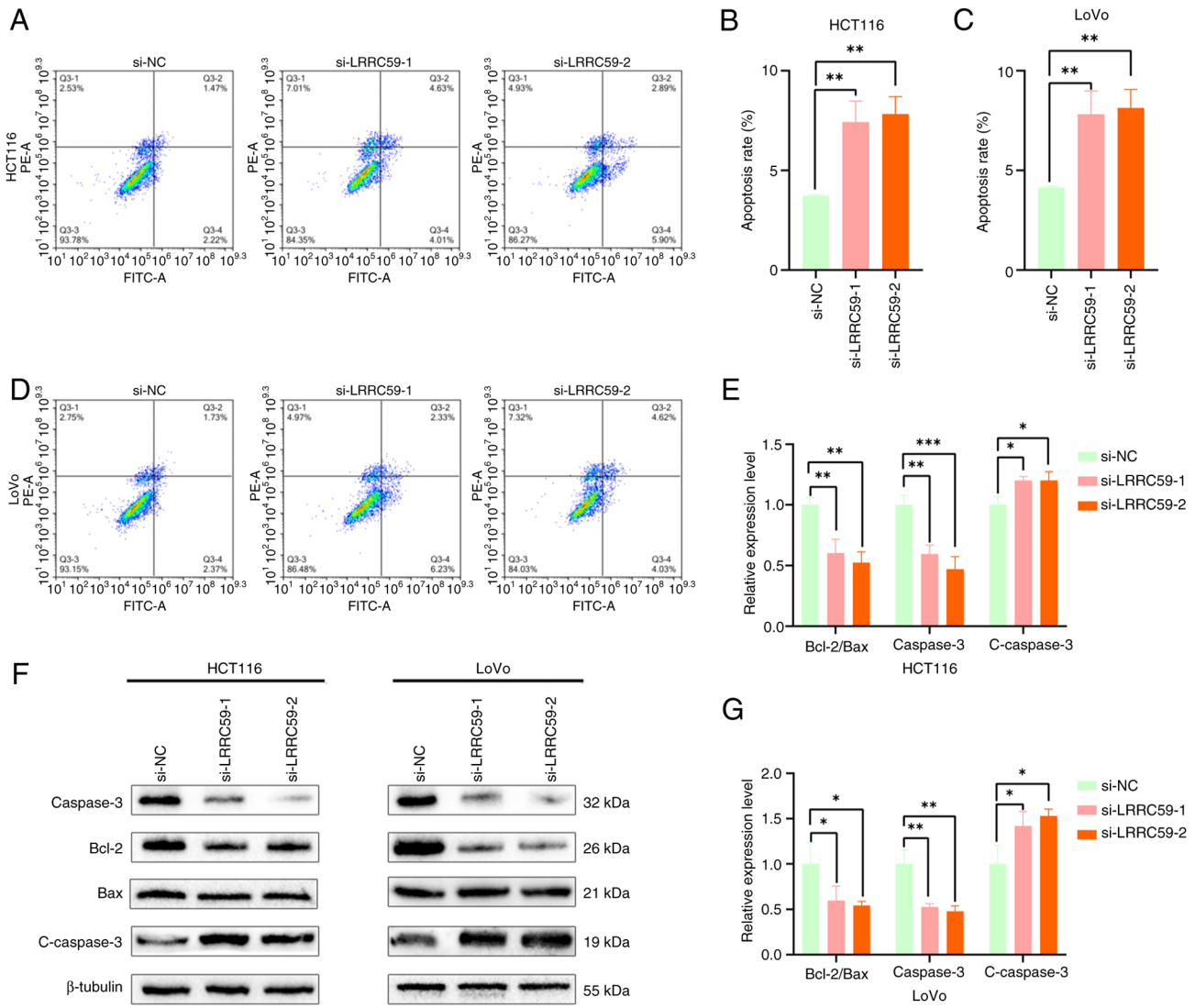

Figure 5. LRRC59 suppresses apoptosis in colorectal cancer cells. (A-D) Flow cytometry of apoptosis in LRRC59 knockdown HCT116 and LoVo cells. (E-G) Western blot analysis of apoptosis-related proteins (Bcl-2, Bax, Caspase3 and active-caspase3) in transfected cells. *P<0.05, **P<0.01 and ***P<0.001. si-, small interfering; NC, negative control.

analysis (Fig. 6A-C) revealed decreased expression of ERS pathway proteins and a reduction in apoptosis-related proteins, including active-caspase-3, whereas the anti-apoptotic protein Bcl-2 was upregulated. Flow cytometry (Fig. 6D-G) confirmed a significant reduction in apoptosis following GSK treatment. These findings suggested that LRRC59 regulates apoptosis by modulating the PERK signaling pathway in CRC cells.

LRRC59 knockdown reduces tumor growth in mice. The effect of LRRC59 on CRC tumorigenesis was assessed *in vivo* in a mouse xenograft model. Western blot analysis confirmed the successful establishment of stable LRRC59-knockdown LoVo cells prior to implantation (Fig. 7A and B). Mice injected with sh-LRRC59 transfected LoVo cells exhibited significantly smaller tumor volumes and weights than the controls (Fig. 7C-E and G). Body weight remained consistent across groups (Fig. 7F). IHC analysis demonstrated increased activation of the PERK pathway in sh-LRRC59 tumors (Fig. 7H and I). These results indicated that LRRC59 knockdown hinders CRC progression by activating the PERK pathway.

Discussion

The role of LRRC59 in CRC progression was investigated. The present findings revealed notable upregulation of LRRC59 expression in CRC tissues, leading to the promotion of cell proliferation, migration and invasion. Additionally, LRRC59 inhibited apoptosis by modulating the PERK signaling. These results suggested that LRRC59 can be used as target for the treatment of CRC.

LRRC59 is a 244-amino acid protein localized to the ER membrane that was initially identified as a ribosome-binding protein (4-6). It is involved in various cellular functions, including immune responses, anti-inflammatory activities, and the translation and translocation of proteins within the ER (28). Previous studies highlighted the involvement of LRRC59 in multiple cancer types (7-9,29,30). However, its role in CRC remains unclear. A recent study suggested that LRRC59 suppresses CRC progression (31), which contrast the current findings. It was found that LRRC59 mRNA expression was significantly higher in CRC tissues than in adjacent

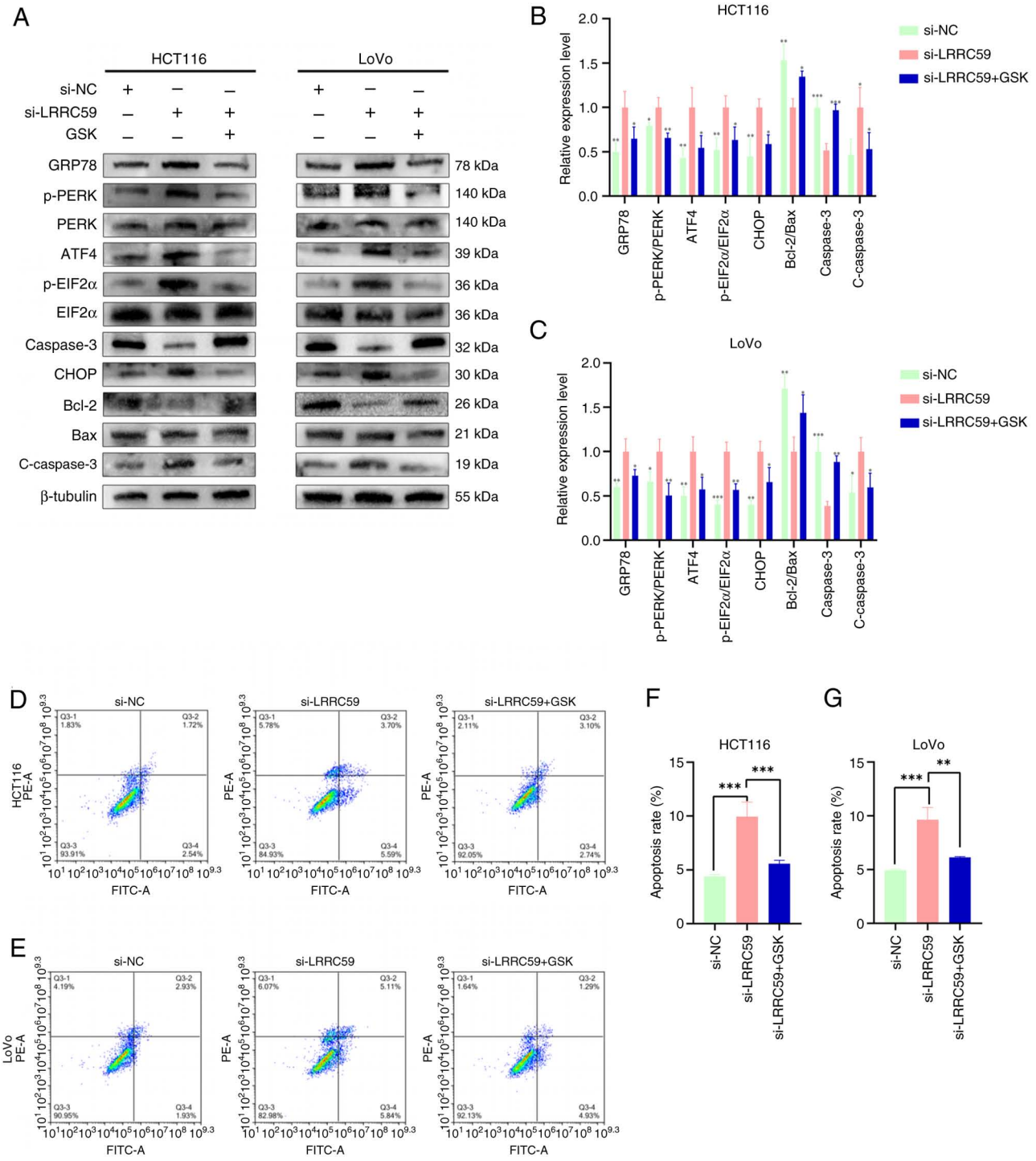

Figure 6. LRRC59 inhibits apoptosis in colorectal cancer cells by suppressing the PERK-mediated ERS signaling pathway. LRRC59 knockdown HCT116 and LoVo cells were treated with GSK (1 μM). (A-C) Expression of PERK-mediated ERS signaling proteins and apoptosis-related proteins was detected by western blot analysis. (D-G) Flow cytometric analysis of apoptosis. *P<0.05, **P<0.01 and ***P<0.001. ER, endoplasmic reticulum; PERK, protein kinase RNA-like ER kinase; ERS, ER stress; p-, phosphorylated; si-, small interfering; NC, negative control.

normal tissues. Subsequent analyses confirmed its overexpression at the protein level in CRC tissues. Furthermore, silencing of LRRC59 reduced CRC cell proliferation and impaired cell migration and invasion. Additionally, LRRC59 knockdown significantly attenuated tumor growth in a mouse xenograft model. These findings suggest that LRRC59 is significantly overexpressed in CRC and plays a key role in promoting CRC progression by inhibiting apoptosis.

The leucine-rich repeat domain of LRRC59 mediates protein-protein interactions, which influence processes such as apoptosis, autophagy and nuclear mRNA transport (32). Previous studies demonstrated that LRRC59 interacts with FGF1 to promote its nuclear import; inhibit apoptosis; and regulate tumor cell survival, proliferation and migration (33,34). Additionally, LRRC59 knockdown induced G1 cell cycle arrest, thereby inhibiting tumor progression.

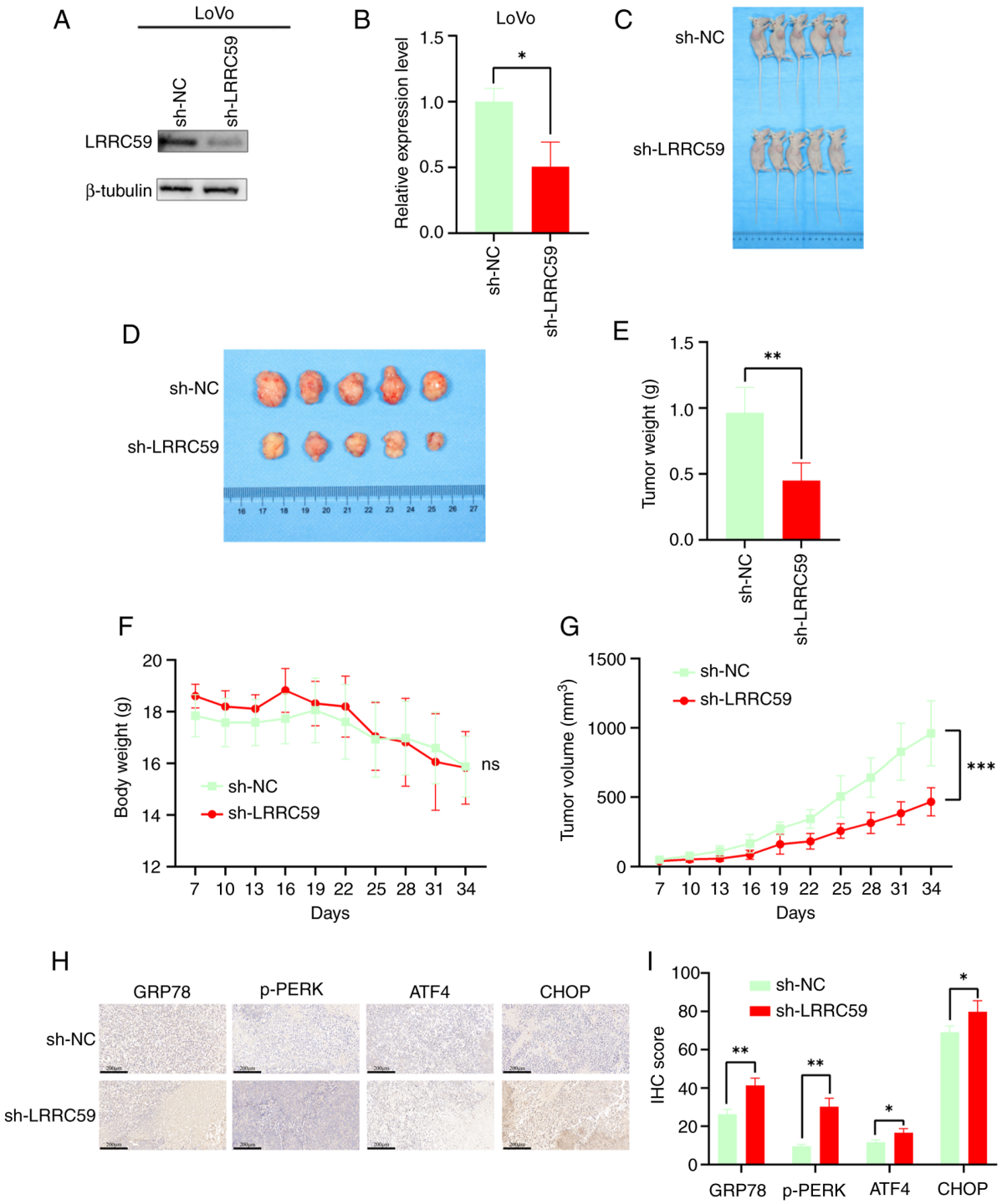

Figure 7. LRRC59 enhances colorectal cancer progression in mouse models. (A and B) Western blot analysis of LRRC59 expression in sh-NC and sh-LRRC59 LoVo cells. (C and D) Images of mice and tumors from sh-NC and sh-LRRC59 groups. (E and G) Tumor volumes measured every 3 days; final tumor weights recorded after 34 days. (F) Body weight trends remained unchanged. (H and I) Immunohistochemistry analysis of PERK pathway activation. Scale bar, 200 μm. *P<0.05, **P<0.01 and ***P<0.001. ER, endoplasmic reticulum; PERK, protein kinase RNA-like ER kinase; sh-, short hairpin; NC, negative control; p-, phosphorylated; ns, non-significant.

In the present study, silencing of LRRC59 elevated apoptotic markers such as active-caspase-3 in CRC cells and decreased expression of the anti-apoptotic protein Bcl-2. These results suggested that LRRC59 suppresses apoptosis in CRC cells.

Malignant tumor progression is characterized by uncontrolled cell proliferation, which creates a highly metabolic, hypoxic, nutrient-deficient and acidic microenvironment. This environment activates the UPR, which amplifies the ERS (35,36). ERS is a dynamic process that responds to protein imbalances in the ER by activating the IRE1-, PERK- and ATF6-mediated ERS pathways during CRC development, thus helping to restore ER homeostasis and support cell survival (37). These pathways initially reduce protein overload in the ER through mechanisms such as PERK-mediated EIF2α phosphorylation, IRE1-dependent mRNA decay, and autophagy activation via the IRE1α-JNK

axis. UPR transcription factors activate ATF6 and splice XBP1 to promote adaptive responses, restore ER function, and support cell survival (38-43). However, if ERS persists, the cells shift from an adaptive response to a death-inducing response (44,45). Numerous studies indicated that the overactivation of the ERS signaling promotes apoptosis, autophagy and ferroptosis in tumor cells (46-50). When ERS conditions are prolonged, IRE1α recruits TRAF2, activating ASK1 and JNK to promote apoptosis (51). Sustained PERK signaling induces apoptosis by upregulating CHOP, a pro-apoptotic transcription factor that downregulates BCL-2 and induces BH3-only protein expression, leading to cell death (52). LRRC59 affects HYOU1- and XBP1-mediated ERS signaling and promotes cancer cell proliferation and migration. However, whether LRRC59 plays a role in CRC via the ERS pathway remains unclear. An association between LRRC59 and the expression of key proteins involved in the PERK-mediated ERS pathway was identified. In CRC cell lines with LRRC59 knockdown, expression of GRP78, p-PERK, p-EIF2α, ATF4 and CHOP was increased. To confirm whether LRRC59 affects apoptosis through the PERK-mediated ERS pathway, the PERK pathway-specific inhibitor GSK was used, which resulted in reduced apoptosis of CRC cells, increased expression of Bcl-2, and decreased expression of active-caspase-3. These findings suggested that LRRC59 inhibits apoptosis and promotes CRC cell survival by suppressing excessive activation of the PERK-mediated ERS signaling pathway.

Given that the PERK pathway plays a central role in the ERS response in CRC cells, targeting the PERK pathway for the treatment of CRC may have broad application prospects (36). Numerous drugs or compounds capable of directly acting on ER-associated proteins have been discovered (53). For instance, V8, a novel derivative of the natural flavonoid wogonin and a potential anticancer agent, has demonstrated significant antitumor activity both *in vitro* and *in vivo*. *In vitro* studies using acute myeloid leukemia cell lines showed that V8 selectively activates the PERK pathway, ultimately triggering CHOP-mediated apoptosis via an ERS-specific pathway (54). Terpenoids, one of the largest and most structurally diverse classes of natural compounds, have been shown in some studies to reduce the incidence of cervical cancer and promote cancer cell apoptosis through the PERK pathway (55). 2-Deoxyglucose, a glucose analog, has been found to exert antitumor effects by promoting the PERK pathway; when combined with HCQ, it can further inhibit the viability and migration of breast tumor cells and induce apoptosis (56). However, the vast majority of currently identified compounds or drugs that may act against tumors via the PERK pathway are still confined to preclinical studies, and their translation into clinical therapies requires further validation through clinical trials. Recent research suggests that cancer treatment strategies employing nanoparticles to target the ER and regulate programmed cell death may represent a promising new direction for clinical translation (57). In the field of nasopharyngeal carcinoma, relevant *in vitro* studies have been conducted: A photothermal nano-vaccine based on phenylboronic acid-modified poly dendrimers of generation 5 attached with indocyanine green can serve as a carrier for the ERS-inducing drug toyocamycin, demonstrating satisfactory antitumor efficacy *in vitro* (58). However, direct targeting of the PERK pathway *in vivo* may not be effective and could result in systemic effects (59). PERK inhibition destroys pancreatic cells and osteoblasts, leading to diabetes and severe bone defects (60,61). Therefore, indirectly affecting the PERK pathway through LRRC59 may be a safe approach for treating CRC. Although LRRC59 shows potential as a therapeutic target, the development of inhibitors and related drugs targeting LRRC59 requires further analysis.

Although it was found that LRRC59 can affect CRC cells through the PERK pathway, there were limitations to the present study. The numbers of clinical specimens and animal model samples used were relatively small, and only two CRC cell lines were evaluated, limiting the generalizability of the results. Further studies are needed to expand the number of clinical samples, increase the number of CRC cell lines and animal models, and explore the molecular mechanism of LRRC59 in greater depth to obtain more universally applicable results. The main objective of the present study was to preliminarily validate the effect of LRRC59 knockdown on CRC cells *in vivo* using a mouse xenograft model. Additional studies are necessary to establish *in situ* transplantation and metastasis models to comprehensively examine the effects of LRRC59 on CRC metastasis and the tumor microenvironment. In the present study, focus was addressed on the PERK pathway branch in ERS, and the literature suggests that LRRC59 is related to other branches of ERS (62). Given the complexity of the UPR pathway, future multi-omics analysis is needed to determine whether LRRC59 can affect CRC through the other two main branches, the IRE1α and ATF6 pathways. Although the PERK pathway was established as the main target of LRRC59, the involvement of non-PERK pathways in tumor progression cannot be ruled out. This is an important topic for future research.

In conclusion, the present study demonstrated that LRRC59 is significantly upregulated in CRC tissues, where it enhances cell proliferation, migration and invasion. Moreover, LRRC59 suppresses apoptosis by attenuating PERK-mediated activation of the ERS pathway. Although research on LRRC59 remains in the early stages, further mechanistic explorations and large-scale clinical trials are required. The current findings indicate the potential of LRRC59 as a therapeutic target for CRC.

Acknowledgements

Not applicable.

Funding

The present study was supported by the Natural Science Foundation of Liaoning (grant no. 2024-MS-152).

Availability of data and materials

The data generated in the present study are included in the figures and/or tables of this article.

Authors' contributions

XH and YW contributed to the methodology, validation, and writing of the original draft. YC participated in data

validation. PZ was involved in conceptualization of the study. GW contributed to study conceptualization, writing, review and editing of the manuscript. BLi conducted formal analyses. BLu performed the experiments. HJ provided resources and performed the experiments. SN was responsible for conceptualization, funding acquisition, supervision, and writing, reviewing and editing the manuscript. XH and SN confirm the authenticity of all the raw data. All authors read and approved the final version of the manuscript.

Ethics approval and consent to participate

The present study was conducted in accordance with the Declaration of Helsinki and was approved (approval no. kY2024-136-01) by the Ethics Committee of the Second Affiliated Hospital of Dalian Medical University (Dalian, China). Animal experiments were conducted in accordance with the ARRIVE guidelines and were approved (approval no. 2024167) by the Institutional Animal Care and Use Committee of Wuhan Servicebio Technology Co., Ltd.

Patient consent for publication

Not applicable.

Competing interests

The authors declare that they have no competing interests.

References

1. Siegel RL, Wagle NS, Cercek A, Smith RA and Jemal A: Colorectal cancer statistics, 2023. CA Cancer J Clin 73: 233-254, 2023.
2. Morgan E, Arnold M, Gini A, Lorenzoni V, Cabasag CJ, Laversanne M, Vignat J, Ferlay J, Murphy N and Bray F: Global burden of colorectal cancer in 2020 and 2040: Incidence and mortality estimates from GLOBOCAN. Gut 72: 338-344, 2023.
3. Leowattana W, Leowattana P and Leowattana T: Systemic treatment for metastatic colorectal cancer. World J Gastroenterol 29: 1569-1588, 2023.
4. Ichimura T, Shindo Y, Uda Y, Ohsumi T, Omata S and Sugano H: Anti-(p34 protein) antibodies inhibit ribosome binding to and protein translocation across the rough microsomal membrane. FEBS Lett 326: 241-245, 1993.
5. Ohsumi T, Ichimura T, Sugano H, Omata S, Isobe T and Kuwano R: Ribosome-binding protein p34 is a member of the leucine-rich-repeat-protein superfamily. Biochem J 294: 465-472, 1993.
6. Ichimura T, Ohsumi T, Shindo Y, Ohwada T, Yagame H, Momose Y, Omata S and Sugano H: Isolation and some properties of a 34-kDa-membrane protein that may be responsible for ribosome binding in rat liver rough microsomes. FEBS Lett 296: 7-10, 1992.
7. Pallai R, Bhaskar A, Barnett-Bernodat N, Gallo-Ebert C, Pusey M, Nickels JT Jr and Rice LM: Leucine-rich repeat-containing protein 59 mediates nuclear import of cancerous inhibitor of PP2A in prostate cancer cells. Tumour Biol 36: 6383-6390, 2015.
8. Li D, Xing Y, Tian T, Guo Y and Qian J: Overexpression of LRRC59 is associated with poor prognosis and promotes cell proliferation and invasion in lung adenocarcinoma. Onco Targets Ther 13: 6453-6463, 2020.
9. Pei L, Zhu Q, Zhuang X, Ruan H, Zhao Z, Qin H and Lin Q: Identification of leucine-rich repeat-containing protein 59 (LRRC59) located in the endoplasmic reticulum as a novel prognostic factor for urothelial carcinoma. Transl Oncol 23: 101474, 2022.
10. Chen X and Cubillos-Ruiz JR: Endoplasmic reticulum stress signals in the tumour and its microenvironment. Nat Rev Cancer 21: 71-88, 2021.
11. Walter P and Ron D: The unfolded protein response: From stress pathway to homeostatic regulation. Science 334: 1081-1086, 2011.
12. Hetz C, Zhang K and Kaufman RJ: Mechanisms, regulation and functions of the unfolded protein response. Nat Rev Mol Cell Biol 21: 421-438, 2020.
13. Shore GC, Papa FR and Oakes SA: Signaling cell death from the endoplasmic reticulum stress response. Curr Opin Cell Biol 23: 143-149, 2011.
14. Long D, Chen K, Yang Y and Tian X: Unfolded protein response activated by endoplasmic reticulum stress in pancreatic cancer: Potential therapeutical target. Front Biosci (Landmark Ed) 26: 1689-1696, 2021.
15. Song M and Cubillos-Ruiz JR: Endoplasmic reticulum stress responses in intratumoral immune cells: Implications for cancer immunotherapy. Trends Immunol 40: 128-141, 2019.
16. Geng J, Guo Y, Xie M, Li Z, Wang P, Zhu D, Li J and Cui X: Characteristics of endoplasmic reticulum stress in colorectal cancer for predicting prognosis and developing treatment options. Cancer Med 12: 12000-12017, 2023.
17. Zhou F, Gao H, Shang L, Li J, Zhang M, Wang S, Li R, Ye L and Yang S: Oridonin promotes endoplasmic reticulum stress via TP53-repressed TCF4 transactivation in colorectal cancer. J Exp Clin Cancer Res 42: 150, 2023.
18. Li F, Dong Q, Kai Z, Pan Q and Liu C: CYP8B1 is a prognostic biomarker with important functional implications in hepatocellular carcinoma. Oncol Rep 54: 104, 2025.
19. Ma H, Suleman M, Zhang F, Cao T, Wen S, Sun D, Chen L, Jiang B, Wang Y, Lin F, *et al*: Pirin inhibits FAS-mediated apoptosis to support colorectal cancer survival. Adv Sci (Weinh) 11: e2301476, 2024.
20. Livak KJ and Schmittgen TD: Analysis of relative gene expression data using real-time quantitative PCR and the 2(-Delta Delta C(T)) method. Methods 25: 402-408, 2001.
21. Xu H, Wang T, Nie H, Sun Q, Jin C, Yang S, Chen Z, Wang X, Tang J, Feng Y and Sun Y: USP36 promotes colorectal cancer progression through inhibition of p53 signaling pathway via stabilizing RBM28. Oncogene 43: 3442-3455, 2024.
22. Zhao L, Sun X, Hou C, Yang Y, Wang P, Xu Z, Chen Z, Zhang X, Wu G, Chen H, *et al*: CPNE7 promotes colorectal tumorigenesis by interacting with NONO to initiate ZFP42 transcription. Cell Death Dis 15: 896, 2024.
23. Kim J, Jeong Y, Shin YM, Kim SE and Shin SJ: FL118 enhances therapeutic efficacy in colorectal cancer by inhibiting the homologous recombination repair pathway through survivin-RAD51 downregulation. Cancers (Basel) 16: 3385, 2024.
24. Zhang Z, Wang L, Zhao L, Wang Q, Yang C, Zhang M, Wang B, Jiang K, Ye Y, Wang S and Shen Z: N6-methyladenosine demethylase ALKBH5 suppresses colorectal cancer progression potentially by decreasing PHF20 mRNA methylation. Clin Transl Med 12: e940, 2022.
25. Wu H, Zheng S, Zhang J, Xu S and Miao Z: Cadmium induces endoplasmic reticulum stress-mediated apoptosis in pig pancreas via the increase of Th1 cells. Toxicology 457: 152790, 2021.
26. Lee H, Lee YS, Harenda Q, Pietrzak S, Oktay HZ, Schreiber S, Liao Y, Sonthalia S, Ciecko AE, Chen YG, *et al*: Beta cell dedifferentiation induced by IRE1α deletion prevents type 1 diabetes. Cell Metab 31: 822-836.e825, 2020.
27. Kim TW, Lee SY, Kim M, Cheon C and Ko SG: Kaempferol induces autophagic cell death via IRE1-JNK-CHOP pathway and inhibition of G9a in gastric cancer cells. Cell Death Dis 9: 875, 2018.
28. Pallai R, Bhaskar A, Barnett-Bernodat N, Gallo-Ebert C, Nickels JT Jr and Rice LM: Cancerous inhibitor of protein phosphatase 2A promotes premature chromosome segregation and aneuploidy in prostate cancer cells through association with shugoshin. Tumour Biol 36: 6067-6074, 2015.
29. Maurizio E, Wiśniewski JR, Ciani Y, Amato A, Arnoldo L, Penzo C, Pegoraro S, Giancotti V, Zambelli A, Piazza S, *et al*: Translating proteomic into functional data: An high mobility group A1 (HMGA1) proteomic signature has prognostic value in breast cancer. Mol Cell Proteomics 15: 109-123, 2016.
30. Pan B, Cheng J, Tan W, Wu X, Fan Q, Fan L, Jiang M, Yu R, Cheng X and Deng Y: Pan-cancer analysis of LRRC59 with a focus on prognostic and immunological roles in hepatocellular carcinoma. Aging (Albany NY) 16: 8171-8197, 2024.
31. Chen H, Zhao T, Fan J, Yu Z, Ge Y, Zhu H, Dong P, Zhang F, Zhang L, Xue X and Lin X: Construction of a prognostic model for colorectal adenocarcinoma based on Zn transport-related genes identified by single-cell sequencing and weighted co-expression network analysis. Front Oncol 13: 1207499, 2023.

32. Xian H, Yang S, Jin S, Zhang Y and Cui J: LRRC59 modulates type I interferon signaling by restraining the SQSTM1/p62-mediated autophagic degradation of pattern recognition receptor DDX58/RIG-I. Autophagy 16: 408-418, 2020.
33. Zhen Y, Sørensen V, Skjerpen CS, Haugsten EM, Jin Y, Wälchli S, Olsnes S and Wiedlocha A: Nuclear import of exogenous FGF1 requires the ER-protein LRRC59 and the importins Kpnα1 and Kpnβ1. Traffic 13: 650-664, 2012.
34. Liu N, Zhang J, Sun S, Yang L, Zhou Z, Sun Q and Niu J: Expression and clinical significance of fibroblast growth factor 1 in gastric adenocarcinoma. Onco Targets Ther 8: 615-621, 2015.
35. Oakes SA: Endoplasmic reticulum stress signaling in cancer cells. Am J Pathol 190: 934-946, 2020.
36. Huang J, Pan H, Wang J, Wang T, Huo X, Ma Y, Lu Z, Sun B and Jiang H: Unfolded protein response in colorectal cancer. Cell Biosci 11: 26, 2021.
37. Urra H, Dufey E, Avril T, Chevet E and Hetz C: Endoplasmic reticulum stress and the hallmarks of cancer. Trends Cancer 2: 252-262, 2016.
38. Harding HP, Novoa I, Zhang Y, Zeng H, Wek R, Schapira M and Ron D: Regulated translation initiation controls stress-induced gene expression in mammalian cells. Mol Cell 6: 1099-1108, 2000.
39. Han D, Lerner AG, Vande Walle L, Upton JP, Xu W, Hagen A, Backes BJ, Oakes SA and Papa FR: IRE1alpha kinase activation modes control alternate endoribonuclease outputs to determine divergent cell fates. Cell 138: 562-575, 2009.
40. 4Hollien J, Lin JH, Li H, Stevens N, Walter P and Weissman JS: Regulated Ire1-dependent decay of messenger RNAs in mammalian cells. J Cell Biol 186: 323-331, 2009.
41. Hollien J and Weissman JS: Decay of endoplasmic reticulum-localized mRNAs during the unfolded protein response. Science 313: 104-107, 2006.
42. Lee AH, Iwakoshi NN and Glimcher LH: XBP-1 regulates a subset of endoplasmic reticulum resident chaperone genes in the unfolded protein response. Mol Cell Biol 23: 7448-7459, 2003.
43. Ameri K and Harris AL: Activating transcription factor 4. Int J Biochem Cell Biol 40: 14-21, 2008.
44. Shi Y, Jiang B and Zhao J: Induction mechanisms of autophagy and endoplasmic reticulum stress in intestinal ischemia-reperfusion injury, inflammatory bowel disease, and colorectal cancer. Biomed Pharmacother 170: 115984, 2024.
45. Sisinni L, Pietrafesa M, Lepore S, Maddalena F, Condelli V, Esposito F and Landriscina M: Endoplasmic reticulum stress and unfolded protein response in breast cancer: The balance between apoptosis and autophagy and its role in drug resistance. Int J Mol Sci 20: 857, 2019.
46. Ji X, Chen Z, Lin W, Wu Q, Wu Y, Hong Y, Tong H, Wang C and Zhang Y: Esculin induces endoplasmic reticulum stress and drives apoptosis and ferroptosis in colorectal cancer via PERK regulating eIF2α/CHOP and Nrf2/HO-1 cascades. J Ethnopharmacol 328: 118139, 2024.
47. Qu J, Zeng C, Zou T, Chen X, Yang X and Lin Z: Autophagy induction by trichodermic acid attenuates endoplasmic reticulum stress-mediated apoptosis in colon cancer cells. Int J Mol Sci 22: 5566. 2021.
48. Wang G, Han J, Wang G, Wu X, Huang Y, Wu M and Chen Y: ERO1α mediates endoplasmic reticulum stress-induced apoptosis via microRNA-101/EZH2 axis in colon cancer RKO and HT-29 cells. Hum Cell 34: 932-944, 2021.
49. Piao MJ, Han X, Kang KA, Fernando PDSM, Herath HMUL and Hyun JW: The endoplasmic reticulum stress response mediates shikonin-induced apoptosis of 5-fluorouracil-resistant colorectal cancer cells. Biomol Ther (Seoul) 30: 265-273, 2022.
50. Quan JH, Gao FF, Chu JQ, Cha GH, Yuk JM, Wu W and Lee YH: Silver nanoparticles induce apoptosis via *NOX4*-derived mitochondrial reactive oxygen species and endoplasmic reticulum stress in colorectal cancer cells. Nanomedicine (Lond) 16: 1357-1375, 2021.
51. Urano F, Wang X, Bertolotti A, Zhang Y, Chung P, Harding HP and Ron D: Coupling of stress in the ER to activation of JNK protein kinases by transmembrane protein kinase IRE1. Science 287: 664-666, 2000.
52. Tabas I and Ron D: Integrating the mechanisms of apoptosis induced by endoplasmic reticulum stress. Nat Cell Biol 13: 184-190, 2011.
53. Zhou R, Wang W, Li B, Li Z, Huang J and Li X: Endoplasmic reticulum stress in cancer. MedComm (2020) 6: e70263, 2025.
54. Guo YJ, Zhu MY, Wang ZY, Chen HY, Qing YJ, Wang HZ, Xu JY, Hui H and Li H: Therapeutic effect of V8 affecting mitophagy and endoplasmic reticulum stress in acute myeloid leukemia mediated by ROS and CHOP signaling. FASEB J 39: e70622, 2025.
55. Zhang P, Liu H, Yu Y, Peng S, Zeng A and Song L: Terpenoids mediated cell apoptotsis in cervical cancer: Mechanisms, advances and prospects. Fitoterapia 180: 106323, 2024.
56. Zhou N, Liu Q, Wang X, He L, Zhang T, Zhou H, Zhu X, Zhou T, Deng G and Qiu C: The combination of hydroxychloroquine and 2-deoxyglucose enhances apoptosis in breast cancer cells by blocking protective autophagy and sustaining endoplasmic reticulum stress. Cell Death Discov 8: 286, 2022.
57. Liang L, Zhu Z, Jiang X, Tang Y, Li J, Zhang Z, Ding B, Li X, Yu M and Gan Y: Endoplasmic reticulum-targeted strategies for programmed cell death in cancer therapy: Approaches and prospects. J Control Release 385: 114059, 2025.
58. Liu Z, Deng X, Wang Z, Guo Y, Hameed MMA, El-Newehy M, Zhang J, Shi X and Shen M: A biomimetic therapeutic nanovaccine based on dendrimer-drug conjugates coated with metal-phenolic networks for combination therapy of nasopharyngeal carcinoma: An in vitro investigation. J Mater Chem B 13: 5440-5452, 2025.
59. Yeap JW, Ali IAH, Ibrahim B and Tan ML: Chronic obstructive pulmonary disease and emerging ER stress-related therapeutic targets. Pulm Pharmacol Ther 81: 102218, 2023.
60. Harding HP, Zeng H, Zhang Y, Jungries R, Chung P, Plesken H, Sabatini DD and Ron D: Diabetes mellitus and exocrine pancreatic dysfunction in perk-/- mice reveals a role for translational control in secretory cell survival. Mol Cell 7: 1153-1163, 2001.
61. Zhang P, McGrath B, Li S, Frank A, Zambito F, Reinert J, Gannon M, Ma K, McNaughton K and Cavener DR: The PERK eukaryotic initiation factor 2 alpha kinase is required for the development of the skeletal system, postnatal growth, and the function and viability of the pancreas. Mol Cell Biol 22: 3864-3874, 2002.
62. Yuan Z, Wang Y, Xu S, Zhang M and Tang J: Construction of a prognostic model for colon cancer by combining endoplasmic reticulum stress responsive genes. J Proteomics 309: 105284, 2024.